

Formation of Peptide Nanospheres and Nanofibrils by Metal Coordination

Mikhail V. Tsurkan and Michael Y. Ogawa*

Department of Chemistry and Center for Photochemical Sciences, Bowling Green State University,
Bowling Green, Ohio 43403

Received August 7, 2007; Revised Manuscript Received October 3, 2007

Two amphipathic polypeptides were coordinated to the cis positions of a square planar Pt(II) complex in order to provide the metal center with two noncovalent oligomerization domains. This resulted in the formation of new metal–peptide nanoassemblies which are shown to exist as nanometer-sized spheres and fibrils. Construction of these assemblies was based on the 30-residue polypeptide AQ-Pal14 which was designed for its ability to self-assemble into the common protein oligomerization motif of a noncovalent coiled-coil, and modified to contain a metal-binding 4-pyridylalanine residue at its surface. When AQ-Pal14 was reacted with Pt(en)(NO₃)₂, a new metal–peptide complex was formed in which two AQ-Pal14 peptides were coordinated to a single metal center as determined by sodium dodecylsulfate polyacrylamide gel electrophoresis (SDS-PAGE) and electrospray ionization mass spectrometry (ESI-MS). When the reaction mixture was analyzed under nondenaturing conditions by high performance size exclusion chromatography (HPSEC), it was found that all species present eluted at the column void volume, indicating the formation of very large metal–peptide assemblies. This was verified by multiangle light scattering (MALS) which showed that the metal–peptide assemblies have a weight-averaged molecular mass and *z*-average root-mean-square radius of $M_w = (7 \pm 4) \times 10^6$ g/mol and $R_z = 18 \pm 4$ nm, respectively. The presence of such nanometer scale assemblies was confirmed by transmission electron microscopy and atomic force microscopy which showed the existence of both spherical and fibrillar nanostructures.

Introduction

Much inspiration for the design of supramolecular nanoassemblies draws from biological precedent where combinations of hydrogen-bond, electrostatic, and hydrophobic interactions are used to drive the assembly of macromolecular building blocks into discrete molecular architectures. In proteins, this can be demonstrated by the way different polypeptide sequences fold into the common secondary structure motifs of α -helices, β -sheets, and β -turns, and how these elements may in turn self-oligomerize into higher order structures such as α -helical coiled-coils and β -sheet fibrils. On the basis of this knowledge, growing interest has focused on the fabrication of new types of bioinspired materials using peptides and amino acids as self-assembling building blocks for supramolecular structures. Indeed, the ease of synthesis, relative stability, and functional variability of polypeptides make them particularly attractive for such use and an increasingly diverse array of self-assembling peptide systems has been studied for future application in such diverse fields as microelectronics, tissue engineering, and medicine.^{1–4} Important examples of this kind of peptide-based nanoscale assembly include the cyclic D,L- α -peptides developed by Ghadiri and co-workers which stack to form hollow, open-ended nanotubes,⁵ the use of linear peptides to form a different class of peptide nanotubes by Matsui and co-workers,² and the design of short peptide fragments that assemble into ordered amyloid fibrils similar to those thought to play important roles in Alzheimer's and other neurodegenerative diseases.^{6–8}

As a complement to the above work, an entirely different approach toward the noncovalent organization of nanoscale assemblies has been developed by inorganic chemists working within the field of supramolecular coordination chemistry.^{9–13}

This work exploits the fact that Werner-type coordination compounds are formed by relatively weak, coordinative metal–ligand bond interactions which produce a variety of precise molecular geometries. The incorporation of appropriate bridging ligands into these systems can allow several such coordination units to be linked together in a predetermined fashion in what has been termed the “directional bonding” approach.^{11,14} Such directional assemblies of coordination compounds have produced an exciting family of nanoscale assemblies which includes different kinds of molecular polygons (triangles, squares, pentagons, etc.), multidimensional molecular panels, and molecular grids. Many of these materials have found application in the design of microporous materials for use as chemical sensors,¹⁵ nanoscopic molecular wires,¹⁶ dendritic antenna systems,¹⁷ and molecular pistons.¹⁸

The work to be described in this paper will combine aspects from these two different paradigms of noncovalent self-assembly in order to generate a new class of hybrid, metal–peptide nanoassemblies. In particular, it extends our initial efforts to utilize the directional bonding properties of coordination compounds to orient self-assembling peptide structures.^{19,20} In earlier work by our group, a covalently cross-linked two-stranded α -helical coiled-coil was prepared, called Pal14C19_{ox}, that had metal-binding 4-pyridylalanine residues located on opposite sides of its structure. It was found that reaction of this peptide with *fac*-Re(CO)₃Br₃, having two labile coordination sites adjacent to one another, produces a continuous series of metal–peptide products in which Re complexes were seen to bridge from two to greater than five coiled-coil units in linear chains.¹⁹ Later work showed how modification of the peptide sequence which placed two additional metal-binding sites onto the surface of the coiled-coil produced a metal-bridged four-helix bundle.²⁰ Here, we continue our investigation into how

* E-mail: mogawa@bgsu.edu.

variation of the coiled-coil peptide sequence can alter the morphologies of the resulting metal–peptide nanoassemblies and show how the coordination of self-assembling polypeptides to a single Pt metal center results in the formation of nanometer scale spheres and fibrils.

Experimental Section

Materials. The reagents pyridine, dichloromethane, and β -mercaptoethanol were purchased from the Sigma-Aldrich Company (St. Louis, MO). Dichloro(ethylenediamine)platinum(II) chloride was purchased from Alfa Aesar (Ward Hill, MA). The Fmoc-protected L-amino acid derivatives including 4-pyridylalanine (PAL), 1-[bis(dimethylamino)methylene]-1*H*-benzotriazolium hexafluorophosphate 3-oxide (HBTU), anhydrous 1-hydroxybenzotriazole (HOBt), piperidine, and diisopropylcarbodiimide were purchased from Peptide International Inc. (Louisville, KY). High purity methanol and acetonitrile were purchased from EMD chemicals (Gibbstown, NJ). All reagents were used as received without further purification.

General Methods. All peptide purification and peptide metalation reactions were monitored by reverse-phase high performance liquid chromatography (HPLC) on either a preparative reversed-phase Vydac C-18 column (10 μ M particle size, 22 \times 250 mm²) or a semipreparative Vydac C-18 column (10 μ M particle size, 10 \times 250 mm²). A linear gradient of water/acetonitrile containing 0.1% (v/v) trifluoroacetic acid was used as the mobile phase. The HPLC runs were performed over 90 min using a flow rate of 2 mL/min for semipreparative and 5–6 mL/min for preparative columns. For HPLC separations, the monitoring wavelengths were set at a wavelength range of 210–262 nm. A two-pump system (Waters model 515) equipped with a Waters model 996 diode array detector/spectrophotometer having a 1 cm path length cell was used. The collected peptides were lyophilized, and the purity of the collected peptide was verified by analytical HPLC, matrix assisted laser desorption ionization mass spectrometry (MALDI-MS), and electrospray ionization mass spectrometry (ESI-MS). Absorption spectra were recorded on a Hewlett-Packard 8452A diode array spectrophotometer. MALDI-MS was performed with a Bruker Daltonics Omnisflex mass spectrometer. Electrospray ionization mass spectrometry was performed with a Shimadzu LCMS 2010A instrument. ¹H NMR and ¹H COSY spectroscopy was performed on a Bruker Avance 300 instrument. Circular dichroism spectra were obtained using an Aviv model 202-01 DS circular dichroism spectrometer equipped with a thermoelectric temperature controller.

Peptide Synthesis. The peptide AQ-Pal14 was synthesized using solid-phase methods on an Applied Biosystems model 433A peptide synthesizer using standard Fmoc chemistry. The 0.25 mmol scale protocol with an N-terminal capping protection strategy by acetic anhydride was used. Activation was achieved by 1-[bis(dimethylamino)methylene]-1*H*-benzotriazolium hexafluorophosphate 3-oxide (HBTU) and 1-hydroxybenzotriazole (HOBt) in DMF. Deprotection of the amino acid side chains and cleavage from the resin was performed by reaction with a mixture of trifluoroacetic acid (TFA) (82.5% v/v), phenol (5% v/v), dithiothreitol (DTT) (2.5% v/v), thioanisole (5% v/v), and water (5% v/v) for 2–3 h at room temperature. The crude peptide was then precipitated in cold anhydrous diethyl ether, collected by vacuum filtration, and dried under a vacuum. Final purification was achieved by preparative reversed-phase C18 HPLC as described above.

SDS-PAGE. Discontinuous sodium dodecylsulfate polyacrylamide gel electrophoresis (SDS-PAGE) was performed using a 4% stacking gel (containing acrylamide (37.5:1), 0.5 M Tris buffer (pH 6.8), ddH₂O, ammonium persulfate, and *N,N,N',N'*-tetramethylethylenediamine) and a 16.5% resolving gel (containing 40% acrylamide (37.5:1), 3 M Tris–Cl 0.3% SDS (pH 8.45), glycerol, ddH₂O, APS, TEMED). The gels were prerun for 10 min at 10 mA/gel in a running (bottom) buffer containing 0.1% SDS and 0.1 M Tris base (0.1 M tricine). Samples were loaded in a buffer containing 0.1% SDS and 0.2 M Tris–Cl (pH 8.9). The gels were stained with Coomassie blue containing 0.25% Coomassie R-50, 50% methanol, and 7.5% glacial acetic acid for 10–30

min. The gels were destained in 10% methanol and 10% glacial acetic acid overnight.

High Performance Size Exclusion Chromatography. High performance size exclusion chromatography (HPSEC) was performed on either a Superdex 75 (3–70 kDa) or a Superdex 200 (10–600 kDa) column (GE Healthcare Bio-Sciences) connected to a Waters model 515 pump equipped with a Waters model 996 diode array detector. The peptide samples were eluted using 50 mM KH₂PO₄/100 mM KCl (pH 7) with a 0.2–0.4 mL/min flow rate and monitored by UV detection. The columns were cleaned with 0.5 M sodium hydroxide after every 15–20 runs.

Atomic Force Microscopy. Atomic force microscopy (AFM) was performed at the AFM Core Facility at the Davis Heart and Lung Research Institute and Biomedical Engineering Center of The Ohio State University using a Digital Instrument Multimode atomic force microscope in tapping mode equipped with MikroMasch NSC15 probes. Two different techniques were used to prepare samples for the experiments. In the evaporation technique, samples were prepared at a concentration ranging from 0.1 to 0.005 mg/mL in water. A 2 μ L portion of the solution was spotted onto freshly peeled muscovite mica and air-dried before imaging. In the incubation-rinsing technique, samples were prepared by depositing 100 μ L of a sample solution on freshly cleaved mica. After incubation for 10 min, the samples were rinsed with filtered water and dried under a stream of nitrogen. Sample concentrations ranged from 0.1 to 0.005 mg/mL. All data were analyzed by WSxM Develop 10.0 software and transferred into digital files.

Transmission Electron Microscopy. Transmission electron microscopy (TEM) was performed at the University of Toledo Health Center on a Philips CM 10 transmission electron microscope. Samples (100–5 mM) were applied onto coated grids for 1 min and dried. The dried samples were negatively stained for 30–60 s with 0.5% uranyl acetate.

Static and Dynamic Light Scattering. Static and dynamic light scattering experiments were performed on a Wyatt Technologies (Santa Barbara, CA) miniDAWN Tristar detector. This was set up in-line with a Wyatt Technologies Optilab rEX refractive index detector coupled to a Shimadzu LC-10AT liquid chromatography system with a Shimadzu SPD-10AV UV–vis detector. The value of dn/dc for apo-peptides and metal–peptide complexes was determined by plotting the absolute value of the refractive index of samples with known concentration against the peptide concentration and can be determined by

$$n_{\text{sample}} = (dn/dc)c_{\text{sample}} + n_{\text{H}_2\text{O}}$$

In some cases, sample concentrations were determined directly from the intensity of the UV signals. All light scattering data were analyzed using the manufacturer's Astra V software package.

Results

Design of the Peptide Ligand. The AQ-Pal14 peptide was designed to self-assemble into the protein structure motif of an α -helical coiled-coil. This motif exists as an intertwining of two or more α -helices that is characterized by a specific “knobs into holes” packing of their hydrophobic side chains.²¹ Within the last 15 years, a significant body of work has been developed to show that synthetic coiled-coils can be constructed from amphipathic peptides whose sequences are based on a seven-residue repeat, (*abcdefg*), in which positions “a” and “d” are occupied by hydrophobic amino acids, positions “b”, “c”, and “f” are occupied by hydrophilic residues, and positions “e” and “g” can be filled by oppositely charged residues.²² Such a design drives the formation of coiled-coils by creating a hydrophobic core at the center of the structure which simultaneously exposes the hydrophilic residues to the bulk solvent and allows formation of interchain salt bridges, as shown in Figure 1. In accordance

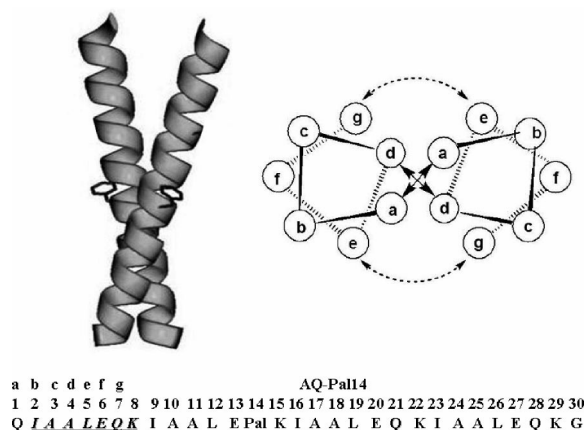


Figure 1. Schematized figure of the two-stranded α -helical coiled-coil formed by AQ-Pal14 (left). Helical wheel diagram of the coiled-coil in which interchain hydrophobic interactions are indicated by the solid arrows and electrostatic interactions between oppositely charged residues are indicated by the hatched arrows (right). The amino acid sequence of the AQ-Pal14 peptide (bottom).

with this general design, solid-phase peptide synthesis was used to prepare AQ-Pal14 having the sequence:



where X is the non-natural amino acid 4-pyridylalanine located at position 14 of the peptide chain. The placement of this residue at the most highly solvent-exposed “f” position of the second heptad repeat was made in order to position metal-binding sites on opposite surfaces of the two-stranded coiled-coil (Figure 1). This design is therefore related to that of the previously studied Pal14C19_{ox} peptide whose 4-pyridylalanine residues were found to react with *fac*-Re(CO)₃Br₃ to form a series of products in which the Re complexes bridged two to greater than five coiled-coil units in linear chains. However, several modifications were made to the sequence of AQ-Pal14. First, weakly hydrophobic alanine residues were incorporated into the heptad “b” positions due to their strong helix-forming tendency which is thought to further stabilize the coiled-coil structure.²⁰ Second, glutamine residues were placed on three of the four heptad “f” positions in order to aid the solubility of the peptide without affecting its surface charge. Third, and perhaps most importantly, the noncovalent nature of the coiled-coil was preserved by eliminating the interchain disulfide bond present in the original Pal14C19_{ox} peptide. Thus, the peptide used in this study was designed to exist as a noncovalent, two-stranded α -helical coiled-coil in which each peptide strand contains a single 4-pyridylalanine metal-binding site on its surface. From this design, it was anticipated that subsequent coordination of two peptide monomers to a single metal center would afford a metal–peptide unit that is able to undergo noncovalent self-assembly through the formation of intermolecular coiled-coils, as shown in Figure 2.

Formation of the Pt–Peptide Building Block Unit. The metal–peptide building blocks were prepared by the incubation of equimolar amounts of apo-peptide and Pt(en)(NO₃)₂ in aqueous solution (H₂O or D₂O) for 1 week at 60 °C. SDS-PAGE was chosen to monitor the course of this reaction because the denaturing conditions of this experiment disrupt the assembly of any noncovalent structures in solution, making this technique selective for observing the presence of the metal–peptide building block units as they are formed. Figure 3 shows that the starting reaction mixture contains only a single peptide

species having a molecular weight of ca. 2.5 kDa which corresponds to that of the peptide monomer. However, within 7 days of reaction, a new species appears having a molecular weight of ca. 4.9 kDa to indicate the formation of a metal–peptide adduct in which two monomeric peptides are coordinated to a single Pt(en) center, as depicted in Figure 2. The assignment of this new species as the Pt complex coordinated to two individual peptide strands is supported by the ESI-MS spectrum of the reaction mixture which contains peaks at m/z = 1138, 975, 853, and 759 which are within experimental error to the 6+, 7+, 8+, and 9+ ions of the disubstituted Pt(en)(peptide)₂ complex (data not shown). Additional peaks in the spectrum occur at m/z = 1096, 822, and 658 and are assigned to the 3+, 4+, and 5+ ions of the apo-peptide. Significantly, no evidence for the monosubstituted Pt–peptide products was observed by ESI-MS, consistent with the SDS-PAGE results.

Further evidence for the formation of the Pt–peptide building block unit was obtained by 2D NMR. Figure 4 shows the ¹H–¹H COSY spectra of the reaction mixture taken after different times of reaction. At first, strong coupling is observed between the protons ortho and meta to the heterocyclic nitrogen atom of the 4-pyridylalanine residues of the peptide which appear at 8.76 and 8.03 ppm, respectively. However, during the course of this reaction, a new cross-peak appears between resonances located at 8.55 and 7.18 ppm, indicating that the pyridyl resonances are shifted upfield upon Pt coordination.

Self-Assembly of Pt–Peptide Building Block Units. As the formation of the metal–peptide building blocks monitored by the above NMR studies was conducted in D₂O, it is interesting to note that broad, unresolved peaks were observed in the amide regions of the one-dimensional ¹H NMR spectra (not shown), even after 7 days of reaction. The absence of amide/solvent exchange in these samples indicates that their amide protons are somehow protected from the bulk solvent and provides the first evidence to indicate the metal–peptide building blocks do indeed self-assemble under nondenaturing conditions. These results are consistent with the circular dichroism spectrum of the Pt–peptide building block units taken in H₂O which consists of minima at 208 and 222 nm having a ratio of $\theta_{222}/\theta_{208}$ = 1.04 to indicate that they do indeed assemble through the formation of coiled-coils.

A further probe of the noncovalent assembly of the metal–peptide building block units was obtained by high performance size exclusion chromatography (HPSEC) performed under nondenaturing conditions. Figure 5 shows the time evolution of the assembly process during the reaction of the peptide and Pt(en)(NO₃)₂ in H₂O. At the start of the reaction, a single well-resolved peak is observed having a retention time of ca. 45 min, which is identical to that of the pure apo-peptide (Figure 5a). The reaction mixture was then seen to elute as an extremely broad, unresolved band after 3 days of reaction (Figure 5b). Since the NMR and SDS-PAGE studies show that the metal–peptide building blocks form within several days of reaction, these HPSEC results indicate that the self-assembly of these units into a mixture of structures having a broad distribution of molecular weights. This assembly process was allowed to continue for 7 days at which time the HPSEC results show that all species present in the solution elute with the void volume of the column and thus have molecular weights in excess of 600 kDa.

Multiangle light scattering (MALS) provides a means for directly measuring both the weight-average molar mass (M_w) and the z-average root-mean-square radius (R_z) of macromolecules by detecting the angle dependent Rayleigh ratio (R_θ) CDV

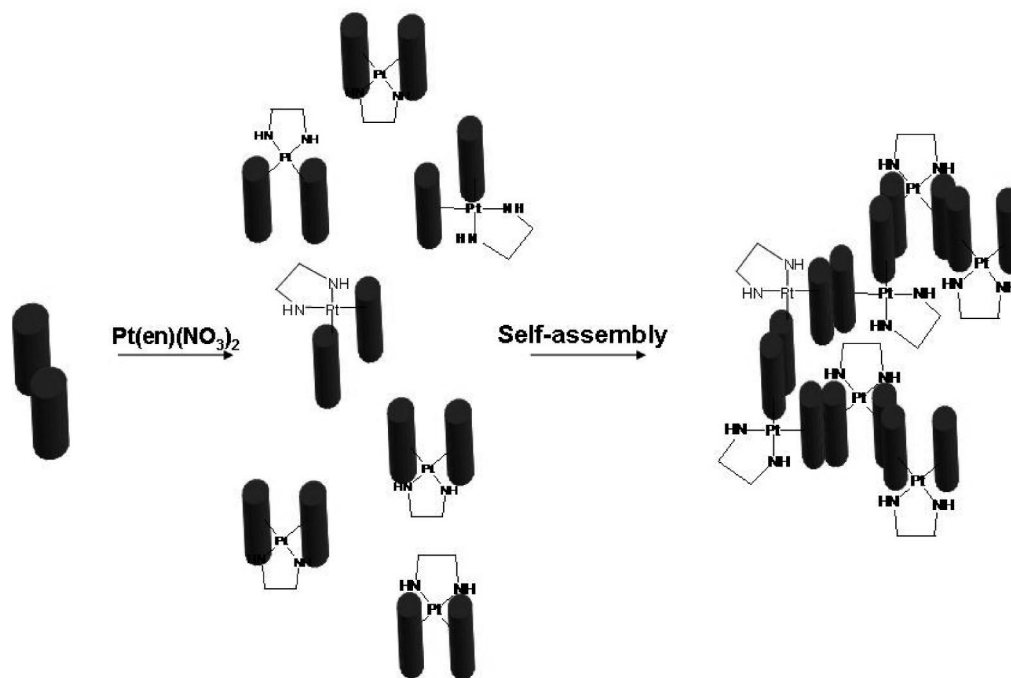


Figure 2. Scheme showing the formation of the metal–peptide building block units via complexation of two AQ-Pal14 peptides (cylinders) to a Pt(en) center and their subsequent self-assembly through the formation of α -helical coiled-coils.

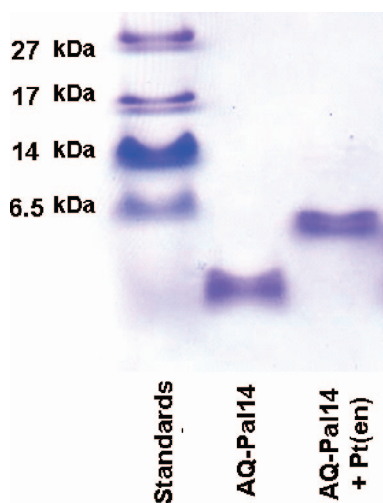


Figure 3. SDS-PAGE of AQ-Pal14 and a stoichiometric mixture of AQ-Pal14 and $\text{Pt(en)}(\text{NO}_3)_2$ after incubation at 60 °C for 7 days.

their scattered light intensity.²³ Equation 1 shows that in the limit of dilute concentrations and small detection angles (or in cases where R_z is small as compared to the incident wavelength), R_θ depends on both M_w and R_z , where K is a constant describing the optical properties of the analyte, c is the weight concentration of the analyte, and θ is the scattering angle.

$$R_\theta = KcM[1 - (16\pi^2/3\lambda^2)\langle R_z^2 \rangle \sin^2(\theta/2)] \quad (1)$$

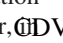
Figure 6 shows a Zimm plot of the data taken from a representative time slice of the HPSEC elution profile for a sample of metal–peptide building blocks annealed for 7 days. As seen, the plot of Kc/R_θ versus $\sin^2(\theta/2)$ follows a straight line which can be used to yield values of M_w and R_z according to eq 1. When averaged over the entire chromatogram, the MALS data give values of $M_w = (7 \pm 4) \times 10^6$ g/mol and $R_z = 18 \pm 4$ nm.

The morphology of the Pt–peptide assemblies was characterized by both transmission electron microscopy (TEM) and

atomic force microscopy (AFM). Both techniques showed the presence of two distinct classes of nanostructures (Figure 7). The dominant population consists of globular structures having diameters in the range 30–50 nm and heights in the range 5–10 nm. These structures have the appearance of collapsed spheres, and it is noted that their diameters are consistent with those determined by the static light scattering experiments described above in which $R_z = 18$ nm. In addition to these spherical structures, Figure 7 shows that the assembly of the Pt–peptide building block units also forms a smaller population of one-dimensional fibrils which have lengths on the order of several hundred nanometers and thicknesses ranging from 4 to 10 nm. It is noted that the presence of both spherical globules and fibrils of these dimensions is reminiscent of the behavior seen when amyloid-forming peptides implicated in the pathology of prion diseases such as Alzheimer's disease self-aggregate under quiescent⁶ conditions and in the presence of Cu^{2+} .⁸

Discussion

There is growing interest in the use of transition metal ions to aid in the assembly of biomolecular nanomaterials. Significant work in this area of research includes the coordination of transition metals to non-natural DNA and PNA nucleosides in order to form new hybridization motifs that do not rely on traditional Watson–Crick base pairing.^{24–26} The importance of such work is that it demonstrates how metal coordination can be used to augment our ability to prepare new types of nanometer scale supramolecular assemblies having potentially predetermined structures. An interesting application of this is the recent fabrication of metallo–DNA assemblies which contain one-dimensional arrays of metal ions for potential application as molecular wires or one-dimensional magnets.^{27,28}

In relation to the preparation of such metallo–DNA materials, transition metals have also been used to direct the assembly of supramolecular polypeptide assemblies for potential application as disease models^{6–8} nanoscale materials.^{19,20,29,30} However, 

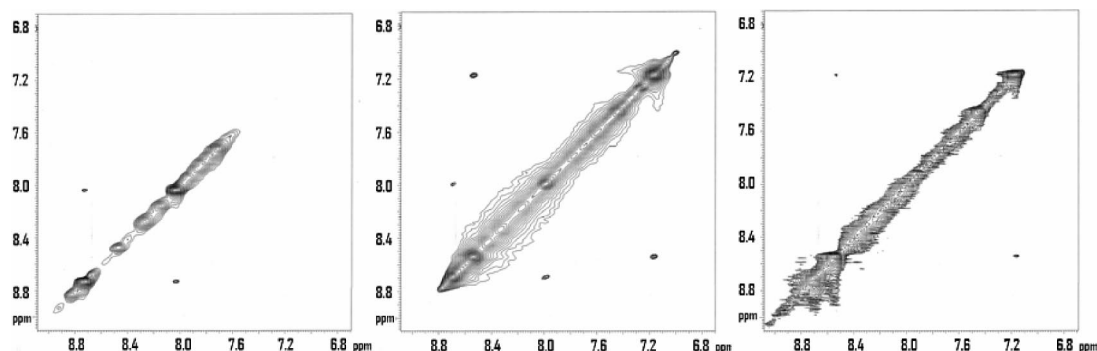


Figure 4. 2D COSY spectra of the reaction mixture taken after (a) 0, (b) 3, and (c) 7 days in D_2O .

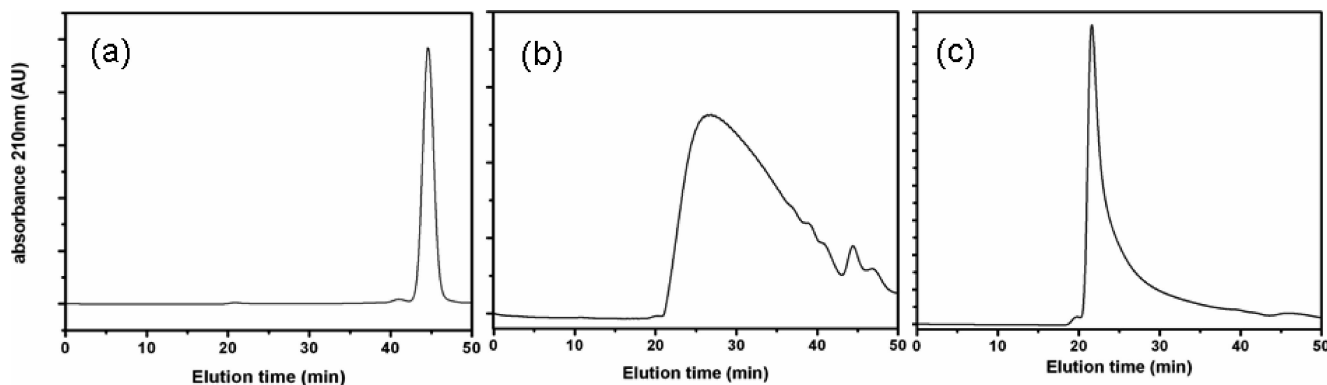


Figure 5. HPSEC behavior of the reaction mixture containing AQ-Pal14 with $Pt(en)(NO_3)_2$ after (a) 0, (b) 3, and (c) 7 days.

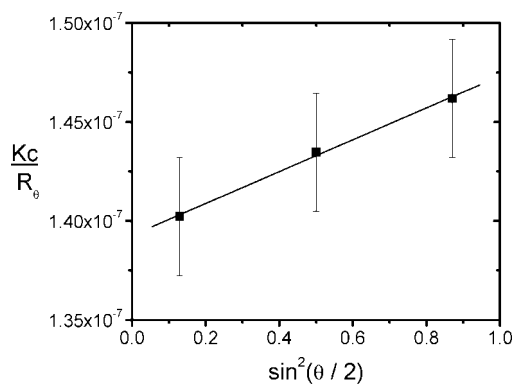


Figure 6. Zimm plot showing the angle dependence of the scattered light intensity from a representative time slice of the HPSEC elution peak.

contrast to DNA, the conformational flexibility of polypeptides contributes to the complexity of understanding how metal coordination can be used to direct the assembly of well-defined three-dimensional structures which may, or may not, exist in nature. From this structural point of view, it is noted that peptide chemists³¹ have long been interested in using transition metals as a means of stabilizing and/or inducing the folding of such discrete secondary protein structure motifs as α -helices³² and β -sheets in small molecule systems.³³

This approach was expanded to create a new class of synthetic metalloproteins which utilize Tris-chelates of transition metal complexes to template the formation of multihelical peptide bundles.^{34,35} These were further developed to create a new class of model redox proteins³⁶ and synthetic ligand-binding proteins.³⁷ More recently, much work within the field of metalloprotein design has focused on the use of naturally occurring amino acids to create metal-binding domains which can be used to assist in the assembly of well-defined protein structures. Examples of systems that exhibit such metal induced folding

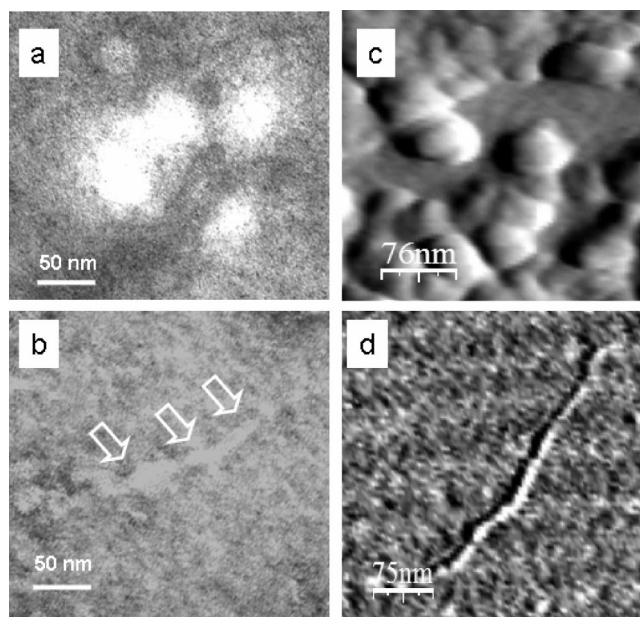


Figure 7. (a, b) Transmission electron micrographs of the two major morphologies of the Pt-peptide assemblies. (c, d) Atomic force micrographs of similar assemblies.

properties to form nativelike structures include the $Cd(II)$ ³⁸ and $Cu(I)$ ³⁹ induced formation of two- and four-stranded α -helical coiled-coils, the latter of which displays unusual photoinduced electron-transfer properties,⁴⁰ the $Hg(II)$ and $Cd(II)$ assisted formation of cysteine-containing three-stranded coiled-coils,^{41,42} and the formation of a histidine-containing triple-helix bundle by $Ni(II)$ binding.⁴³

The results described in this paper complement the studies discussed above by exploring the use of metal coordination to prepare new types of molecular architectures which do not ex-

in nature. Here, a new type of metal–peptide building block was prepared in which two AQ-Pal14 peptides were coordinated to the cis positions of a single Pt(en)²⁺ center. The peptides used in this way were designed to self-assemble into α -helical coiled-coils, and their coordination to the Pt(en) center was expected to provide it with two noncovalent oligomerization domains oriented 90° from one another. It was shown by a variety of techniques that these metal–peptide building blocks do indeed self-assemble in aqueous solution by the formation of coiled-coils, and that the resulting assemblies exist as large spherical arrays having diameters in the range 30–50 nm both in solution and on solid substrates.

At this point, it is of interest to compare the conformational properties of the assemblies formed by the reaction of Pt(en)(NO₃)₂ and AQ-Pal14 with those of related assemblies prepared in our laboratory. Our earliest attempt to use metal coordination to direct the assembly of peptide structures involved the reaction of the peptide Pal14C19_{ox} with *fac*-Re(CO)₃Br₃.¹⁹ The main difference in this peptide was that its dimeric coiled-coil structure was rigorously enforced by the presence of an interchain disulfide cross-link between cysteine residues located in the hydrophobic core of the coiled-coil. It was observed that coordination of Pal14C19_{ox} to the cis positions of the Re(CO)₃Br core produced a continuous series of metal–peptide products in which Re complexes bridged from two to greater than five coiled-coil units in linear chains. No evidence for formation of nanospheres or nanofibrils was observed in those assemblies. In addition, more recent work from our laboratory examined the products formed when AQ-Pal14Pal21 was reacted with Pt(en)(NO₃)₂. This peptide does not contain a disulfide cross-link, and thus retains the noncovalent nature of the coiled-coil, but does possess two pyridylalanine metal-binding domains on its surface. It was observed that the resulting metal–peptide assembly existed as a discrete four-helix bundle in which four Pt centers were presumably bound to its surface to stabilize this assembly. Together, these results suggest the interesting possibility that the conformational flexibility of the metal–peptide building blocks might favor the formation of large nanoassemblies. Nanospheres and fibrils are formed when the most conformationally flexible AQ-Pal14 peptide is reacted with Pt(en)(NO₃)₂, discrete four-helix bundles are formed when two metal complexes are used to cross-link the AQ-Pal14Pal21 peptides, and short metal–peptide oligomers result when the most conformationally rigid Pal14C19_{ox} peptides are coordinated to a single metal center. It is hoped that further investigation into the formation of these metal–peptide supramolecular assemblies will produce additional insight into ways of fabricating new bioinspired nanomaterials.

Acknowledgment. This work was supported by NSF Grant No. CHE-0455441 and ACS-PRF Grant No. 40790-AC. M.V.T. acknowledges the receipt of a Helen and Harold McMaster Predoctoral Fellowship. The authors thank Prof. William Gunning at the University of Toledo Health Science Center for assistance in obtaining the transmission electron micrographs and Mr. Ron Myers of Wyatt Technology Corporation for helpful discussions. Reviewer 1 is thanked for providing insightful comments regarding this system.

References and Notes

- (1) Reches, M.; Gazit, E. *Curr. Nanosci.* **2006**, 2, 105.
- (2) Gao, X. Y.; Matsui, H. *Adv. Mater.* **2005**, 17, 2037.
- (3) Rajagopal, K.; Schneider, J. P. *Curr. Opin. Struct. Biol.* **2004**, 14, 480.
- (4) Zhang, S. G. *Nat. Biotechnol.* **2003**, 21, 1171.
- (5) Bong, D. T.; Clark, T. D.; Granja, J. R.; Ghadiri, M. R. *Angew. Chem. Int. Ed.* **2001**, 40, 988.
- (6) Moore, R. A.; Hayes, S. F.; Fischer, E. R.; Priola, S. A. *Biochemistry* **2007**, 46, 7079.
- (7) Ghosh, S.; Verma, S. *Tetrahedron Lett.* **2007**, 48, 2189.
- (8) Smith, D. P.; Ciccotosto, G. D.; Tew, D. J.; Fodero-Tavoletti, M. T.; Johanssen, T.; Masters, C. L.; Barnham, K. J.; Cappai, R. *Biochemistry* **2007**, 46, 2881.
- (9) Sun, S. S.; Lees, A. J. *Coord. Chem. Rev.* **2002**, 230, 171.
- (10) Fujita, M.; Umemoto, K.; Yoshizawa, M.; Fujita, N.; Kusukawa, T.; Biradha, K. *Chem. Commun.* **2001**, 509.
- (11) Holliday, B. J.; Mirkin, C. A. *Angew. Chem. Int. Ed.* **2001**, 40, 2022.
- (12) Leininger, S.; Olenyuk, B.; Stang, P. J. *Chem. Rev.* **2000**, 100, 853.
- (13) Slone, R. V.; Benkstein, K. D.; Belanger, S.; Hupp, J. T.; Guzei, I. A.; Rheingold, A. L. *Coord. Chem. Rev.* **1998**, 171, 221.
- (14) Seidel, S. R.; Stang, P. J. *Acc. Chem. Res.* **2002**, 35, 972.
- (15) Mines, G. A.; Tzeng, B. C.; Stevenson, K. J.; Li, J. L.; Hupp, J. T. *Angew. Chem. Int. Ed.* **2002**, 41, 154.
- (16) Schlicke, B.; Belsler, P.; De Cola, L.; Sabbioni, E.; Balzani, V. *J. Am. Chem. Soc.* **1999**, 121, 4207.
- (17) Balzani, V.; Ceroni, P.; Juris, A.; Venturi, M.; Campagna, S.; Puntoriero, F.; Serroni, S. *Coord. Chem. Rev.* **2001**, 219, 545.
- (18) Ashton, P. R.; Balzani, V.; Kocian, O.; Prodi, L.; Spencer, N.; Stoddart, J. F. *J. Am. Chem. Soc.* **1998**, 120, 11190.
- (19) Tsurkan, M. V.; Ogawa, M. Y. *Chem. Commun.* **2004**, 2092.
- (20) Tsurkan, M. V.; Ogawa, M. Y. *Inorg. Chem.* **2007**, 46, 6849.
- (21) Burkhard, P.; Stetefeld, J.; Strelkov, S. V. *Trends Cell Biol.* **2001**, 11, 82.
- (22) Hodges, R. S. *Biochem. Cell Biol.* **1996**, 74, 133.
- (23) Andersson, M.; Wittgren, B.; Wahlund, K. G. *Anal. Chem.* **2003**, 75, 4279.
- (24) Tanaka, K.; Shionoya, M. *J. Org. Chem.* **1999**, 64, 5002.
- (25) Popescu, D. L.; Parolin, T. J.; Achim, C. *J. Am. Chem. Soc.* **2003**, 125, 6354.
- (26) Weizman, H.; Tor, Y. *J. Am. Chem. Soc.* **2001**, 123, 3375.
- (27) Clever, G. H.; Carell, T. *Angew. Chem. Int. Ed.* **2007**, 46, 250.
- (28) Shionoya, M.; Tanaka, K. *Curr. Opin. Chem. Biol.* **2004**, 8, 592.
- (29) Gerhardt, W. W.; Weck, M. *J. Org. Chem.* **2006**, 71, 6333.
- (30) Ohr, K.; McLaughlin, R. L.; Williams, M. E. *Inorg. Chem.* **2007**, 46, 965.
- (31) Schneider, J. P.; Kelly, J. W. *Chem. Rev.* **1995**, 95, 2169.
- (32) Ruan, F. Q.; Chen, Y. Q.; Hopkins, P. B. *J. Am. Chem. Soc.* **1990**, 112, 9403.
- (33) Schneider, J. P.; Kelly, J. W. *J. Am. Chem. Soc.* **1995**, 117, 2533.
- (34) Ghadiri, M. R.; Case, M. A. *Angew. Chem. Int. Ed.* **1993**, 32, 1594.
- (35) Lieberman, M.; Tabet, M.; Sasaki, T. *J. Am. Chem. Soc.* **1994**, 116, 5035.
- (36) Mutz, M. W.; Case, M. A.; Wishart, J. F.; Ghadiri, M. R.; McLendon, G. L. *J. Am. Chem. Soc.* **1999**, 121, 858.
- (37) Moffet, D. A.; Case, M. A.; House, J. C.; Vogel, K.; Williams, R. D.; Spiro, T. G.; McLendon, G. L.; Hecht, M. H. *J. Am. Chem. Soc.* **2001**, 123, 2109.
- (38) Kharenko, O. A.; Ogawa, M. Y. *J. Inorg. Biochem.* **2004**, 98, 1971.
- (39) Kharenko, O. A.; Kennedy, D. C.; Demeler, B.; Maroney, M. J.; Ogawa, M. Y. *J. Am. Chem. Soc.* **2005**, 127, 7678.
- (40) Hong, J.; Kharenko, O. A.; Fan, J. F.; Xie, F.; Petros, A. K.; Gibney, B. R.; Ogawa, M. Y. *Angew. Chem. Int. Ed.* **2006**, 45, 6137.
- (41) Farrer, B. T.; Pecoraro, V. L. *Proc. Natl. Acad. Sci. USA* **2003**, 100, 3760.
- (42) Li, X. Q.; Suzuki, K.; Kanaori, K.; Tajima, K.; Kashiwada, A.; Hiroaki, H.; Kohda, D.; Tanaka, T. *Protein Sci.* **2000**, 9, 1327.
- (43) Suzuki, K.; Hiroaki, H.; Kohda, D.; Nakamura, H.; Tanaka, T. *J. Am. Chem. Soc.* **1998**, 120, 13008.

BM700879T